

Experimental demonstration of emission of solitons from a resonant localized waveXinyun Liu , Xinlong Wang,^{*} Haohua Liu, Shaohua Wang, and Mei Wen*Key Laboratory of Modern Acoustics (MOE) and Institute of Acoustics, Nanjing University, Nanjing 210093, People's Republic of China*

(Received 15 August 2019; accepted 28 September 2020; published 2 November 2020)

We demonstrate the emission of solitons from a resonantly excited localized standing wave in a nonlinear chain of spring-coupled masses. The localized wave in this system is induced by a properly designed “impurity” and vibrates around the “impurity” with an intrinsic frequency. We observe that, when subjected to an external forcing, it is amplified to a large amplitude under the nonlinear resonance, and, then, its wave envelope splits apart leading to the release of most of its energy in the form of a large-amplitude traveling soliton. The experiment also shows that the rate of the emission can be controlled by finely tuning the driving parameters, thereby providing a feasible and controllable way for creation of solitons.

DOI: [10.1103/PhysRevE.102.052201](https://doi.org/10.1103/PhysRevE.102.052201)**I. INTRODUCTION**

Solitons, a kind of traveling localized nonlinear wave objects with constant speed and invariant shapes [1], are formed due to a dynamic balance of interaction between nonlinearity and dispersion. So far there have been extensive studies and a fairly in-depth understanding of the existence, propagation, and interactions of solitons that occur in nature [2–4] and in physical systems [5–16]. However, the internal dynamic mechanism of their formation and creation still remains to be further explored. An understanding of this would make it viable for solitons to be generated in an efficient and controllable way, which would not only be of fundamental value in soliton physics, but also be key to relevant engineering applications.

Although solitons in integrable systems, according to the inverse scattering theory [17], can in principle be evolved from some preset initial conditions [18,19], it seems highly infeasible to precisely set up and control an initial waveform that would definitely evolved into what is desired. Moreover, nonideal factors such as dissipation and environmental disturbances would also make a real physical system nonintegrable. It therefore necessitates the development of approaches that are experimentally realizable for efficient creation of solitons.

One of the few approaches, proposed by Friedland [20,21], was based on a mechanism of autoresonance. It was argued that a specially designed spatial distribution of nonlinear waves would evolved into large-amplitude solitons by using passage through an ensemble of resonances and subsequent multiphase self-locking of the system with perturbations. Another mechanism called nonlinear supratransmission (NST) was uncovered by Geniet and Leon [22–25] in a nonlinear system driven by one end. It was shown when the driving amplitude is large enough, solitonic pulses are emitted due to the nonlinear instability. Although amenable for experiments, this method still faces some problems. For example,

the large-amplitude driving gives rise to the quasilinear wave background, which reduces the purity of the solitons.

The generation of solitons by resonant absorption of electromagnetic wave has been proved to be effective in plasma [26–28]. Driven by an external electric field imposed on a nonuniform plasma, the Langmuir wave near the critical density could be resonantly excited. After the phase of growing the localized electric wave propagates down the density gradient. The periodical emission of solitons in plasma has also been demonstrated numerically [29]. However, the presence of ion inertial disorders the periodic emission process, making it hard to achieve in experiments.

Our group has proposed a scheme for controllable creation of solitons from a resonantly excited localized wave [30]. In this scheme, the localized wave mode, which may be introduced, e.g., by a mass “impurity” in a semi-infinite β -FPU chain, has a unique natural frequency f_r that falls in the linear forbidden band. When subjected to an external drive of frequency $f \approx f_r$, the localized wave mode can be captured into nonlinear resonance leading to an instability that gives rise to the emission of solitary waves. As we demonstrated numerically [30], the driving threshold could be reduced to one-third of that for supratransmission and the efficiency is almost doubled with noise greatly suppressed. Utilizing resonance introduced by a mass “impurity,” the emission rate of solitons could be well controlled by finely tuning the parameter in a wide range.

II. EXPERIMENTAL DESIGN

To demonstrate all these predictions [30], we report our design and implementation of an experimental β -FPU system. We first attempted to realize the β -FPU model simply by an one-dimensional chain (along the x axis) of spring-coupled masses that are placed on a horizontal and smooth table and oscillate *transversely*, as schematically shown in Fig. 1(a). Let ξ_n denote the transverse displacement (in the y direction) of the n th mass M_n in the chain ($n = 0, 1, 2, \dots$) and F_n the elastic force of the spring that is between the $(n - 1)$ -th and

^{*}xlwang@nju.edu.cn

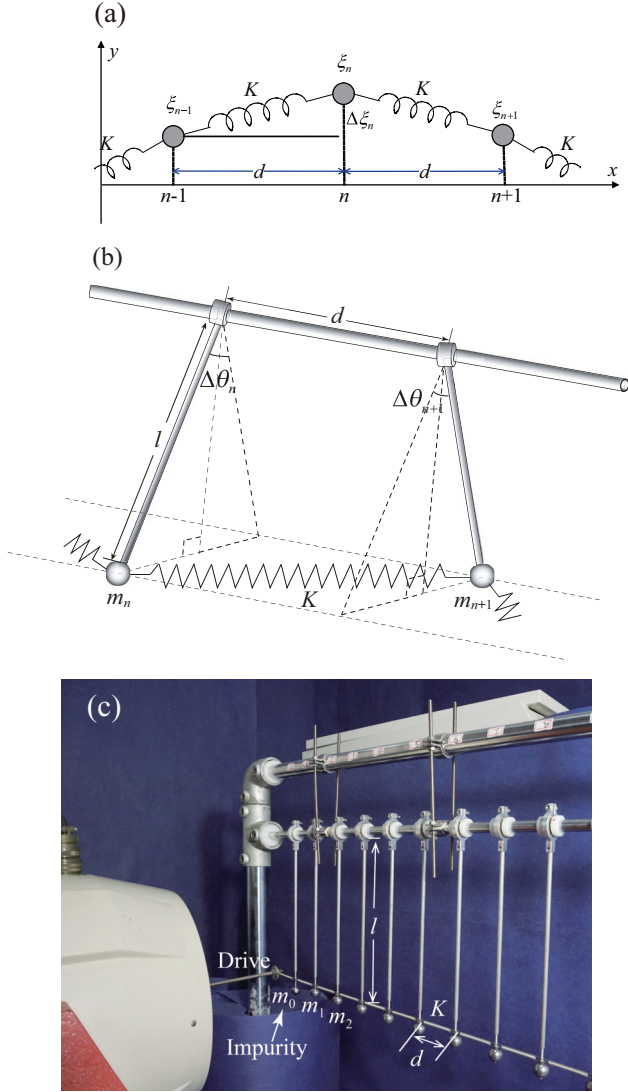


FIG. 1. System design and implementation. (a) Prototype of a transversely vibrating chain of masses coupled by springs, (b) sketch of a single unit of a chain of spring-coupled pendulums, and (c) photograph of the experimental setup.

the n th masses. Every spring in this system is assumed to be linear and has the same elastic coefficient K . It has a relaxed length d_0 and is prestretched to d (the static length in the motionless state), so that $F_n = -K[\sqrt{d^2 + (\Delta\xi_n)^2} - d_0]$, with $\Delta\xi_n \equiv \xi_n - \xi_{n-1}$ being the difference of the transverse displacements of neighboring masses. The transverse projection of F_n is $F_n^\perp = F_n \sin \alpha_n$, with $\tan \alpha_n = \Delta\xi_n/d$ being the slope of the n th spring with respect to the chain axis on the horizontal table. For $|\Delta\xi_n| \ll d$, a cubic approximation yields $F_n^\perp \approx F(\Delta\xi_n)$, where the nonlinear function

$$F(\Delta\xi_n) = -K_1 \Delta\xi_n - \frac{K_3}{2d^2} \Delta\xi_n^3, \quad (1)$$

with

$$K_1 = \frac{d - d_0}{d} K, \quad K_3 = \frac{d_0}{d} K. \quad (2)$$

Note that $d - d_0 = d_1$ is the *prestretch* of the springs that provides the linear part ($K_1 \neq 0$) of the elastic force F . Without it, F would be purely nonlinear [31]. Since $K_1 + K_3 = K$, the relative weight between the linear and nonlinear parts of F is readily adjustable, in particular, both parts can be of comparable order in magnitude, provided that d_1 is properly set. The total transverse force of restoration acting on the n th mass M_n is given by $F_n^\perp - F_{n+1}^\perp \approx F(\Delta\xi_n) - F(\Delta\xi_{n+1})$. Hence, under the assumptions of frictionless and small-amplitude vibration ($|\Delta\xi_n| \ll d$), the equation governing the transverse vibration turns out to be

$$M_n \ddot{\xi}_n \approx K_1 (\Delta\xi_{n+1} - \Delta\xi_n) + \frac{K_3}{2d^2} (\Delta\xi_{n+1}^3 - \Delta\xi_n^3), \quad (3)$$

for $n = 0, 1, 2, \dots$, which is a standard β -FPU model. According to Ref. [30], a mass “impurity” can be introduced, e.g., at site $n = 0$, by setting $M_0 < M$ and $M_{n \neq 0} = M$. It induces a localized wave of a unique intrinsic frequency $f_r = \omega_r/2\pi$. In the linear approximation, it can be proved for $\xi_{-1} = 0$ that

$$\omega_r = \frac{\omega_0/2}{\sqrt{m-1} + \sqrt{1-m}}, \quad \left(m = \frac{M_0}{M}, \omega_0^2 = \frac{4K_1}{M} \right), \quad (4)$$

where the mass ratio m measures the “impurity” and ω_0 is the lower bound of the forbidden band where linear waves are prohibited. It is easily seen that, for $m < 1$, the intrinsic frequency ω_r falls within the forbidden band, i.e., $\omega_r > \omega_0$, and $\omega_r = \omega_0$ if and only if $m = 3/4$.

However, there are two major technical problems that hinder us from implementing the proposed system. The first is how to suppress the effect of friction on mass balls. Our test shows that even if the supporting table is made extremely smooth, the friction between the table and mass balls is still strong enough to soon dissipate energy of vibration. The second is how to maintain the motion of all masses exactly in the required transverse (y) direction. Owing to the nonbalanced longitudinal component of the elastic force, i.e., $F_n \cos \alpha_n \neq F_{n+1} \cos \alpha_{n+1}$, there would exist non-negligible longitudinal (x) displacements of masses, making the resultant equation deviate severely from Eq. (3). Of course, one may set up a transversely guiding track for each mass to force it to move exactly in the y direction on the horizontal plane, but an installed track would introduce additional friction, which further intensifies the friction effect.

We find that both unfavorable effects can effectively be alleviated if masses in the chain are suspended and constrained to move by some long rigid sticks. We then design an improved system that consists of a chain of pendulums, with their massive bobs being hinged with springs and their pivots mounted equidistantly on a horizontal steel beam (with spacing d), as is sketched in Fig. 1(b). The pivots of pendulums are some axle bearings on the steel beam, which effectively constrain the motions of the massive bobs on vertical planes perpendicular to the beam, as long as the hanging rods are stiff enough. The trajectories of the bobs on these vertical planes are almost horizontal, provided that θ_n , the swing angles, are sufficiently small, or the rods (of length l) are sufficiently long as compared to the displacements $\xi_n = l\theta_n$ of the massive bobs. For each of the pendulums, the friction occurs mainly at its pivot, and it attributes a negligible torque as compared

with that of the elastic force provided by coupling springs. We select sufficiently large stiffness of springs, so that the gravitational torque acting upon each pendulum is negligible as compared to the torque generated by the springs (see below). In this way, the swing motion is dominated by the momenta of the elastic forces, rather than what are found in the sine-Gordon type [22,32] and coupled pendulum chains based on torsion and gravity in opposition [33].

The axis component L_n of the momentum owing to the elastic force of the n th spring is derived and can be written as

$$L_n(\Delta\theta_n) = -Kl^2 \left(1 - \frac{d_0}{\sqrt{d^2 + 4l^2 \sin^2 \frac{\Delta\theta_n}{2}}} \right) \sin \Delta\theta_n,$$

where $\Delta\theta_n = \theta_n - \theta_{n-1}$. For $|\Delta\theta_n| \ll 1$, it is approximated that $L_n(\Delta\theta_n) \approx \hat{F}(l\Delta\theta_n)l$, where function $\hat{F}(z)$ has the same form as given in formula (1) but with K_3 replaced by

$$\hat{K}_3 = K_3 - \frac{1}{2} \left(\frac{d}{l} \right)^2 K_1. \quad (5)$$

If the pendulums are so long that $l \gg d$, then $\hat{K}_3 \approx K_3$, and thus, $\hat{F} \approx F$. The swing of the n th pendulum then obeys the equation, $I_n \ddot{\theta}_n \approx L_n - L_{n+1}$, with $I_n = M_n l^2$ being the rotational inertial of the n th pendulum. Here $M_n = m_n + \frac{1}{3} m_{\text{rod}}$ is an effective mass that takes account of the rod mass m_{rod} and the bob mass m_n of the n th pendulum. Applying the approximant of L_n , we obtain the equation for θ_n , which appears in the same form as Eq. (3) if letting $\xi_n = l\theta_n$ and replacing K_3 by \hat{K}_3 .

Based on these considerations, we have built an experimental system composed of an array of 60 pendulums as shown in Fig. 1(c). To support the large load of the pendulums, we install a structure of double steel beams, the upper of which is used to maintain the horizontality of the lower one that hangs pendulums directly with pivots. We adopt an aluminum rod of length $l = 30$ cm and mass $m_{\text{rod}} = 24$ g for each pendulum, and use springs of elastic coefficient $K = 70$ N/m and relaxed length $d_0 = 4$ cm, each prestretched to a static length of $d = 6$ cm when connecting neighboring bobs. The springs also have a factory-set pretension of $F_0 = 0.35$ N, which can serve for the same purpose as the prestretch. It can be shown that Eq. (3) are still valid in the presence of the pretension F_0 , only if d_0 is replaced by $d_0 - F_0/K$ in the definitions of K 's in Eq. (2). A rather tedious analytical estimation shows the gravitational torque upon each pendulum is less than 5% of elastic moment, which meets the requirement of the design. The first pendulum ($n = 0$), which plays the role of ‘‘impurity’’ in the present system, has a lighter mass of $m_0 = 23.06$ g, while other balls weigh $m_{n>0} = 30.21$ g. With these parameters, we calculate from formula (4) that $f_0 = \omega_0/2\pi \approx 8.79$ Hz and $f_r = \omega_r/2\pi \approx 8.88$ Hz. According to our previous work [30], the ‘‘light mass’’ impurity will have the center of the localized wave shift slightly to a position $x_0 > 0$ in our semi-infinite chain. The shift can also be observed in the experiment, as is shown in Fig. 2(a). Thus more energy can be absorbed from the driving, and the center-shifted localized wave is more unstable when it is resonantly amplified even for small driving, leading to the periodic emission of solitons. In the

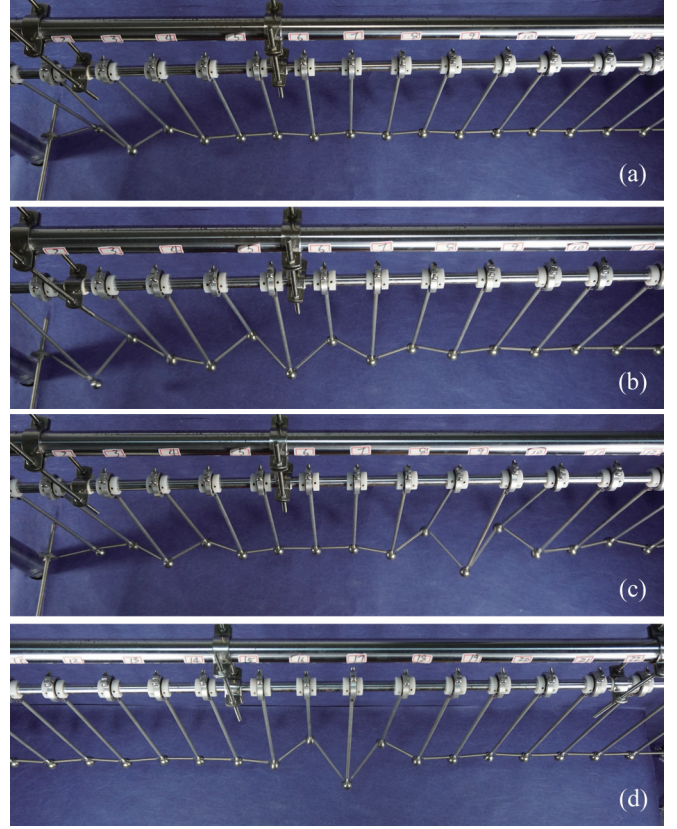


FIG. 2. Snapshots of emission of solitons from the ‘‘impurity’’-induced localized wave around the pendulum next to the drive of displacement $\xi_{-1} = 12.7 \cos 2\pi ft$ mm ($f = 9.33$ Hz). (a) At first, an evanescent wave of small amplitude is stirred up around the drive. (b) The localized wave is amplified with its center slightly moving to the right. (c) The localized wave splits apart, releasing a solitary-wave packet that propagates away. Note that now the ‘‘impurity’’ oscillates in phase with the driving. (d) The soliton is passing through the 17th pendulum.

‘‘heavy mass’’ case, however, the center of solitons is shifted out of our semi-infinite chain ($x < 0$), making it impossible to split a soliton, as has been confirmed both in our numerical simulations and experiments.

An electro-magnetic shaker (Type LDS-V780, B&K) is used to drive the system via the spring that connects the bob of the first pendulum, as shown in Fig. 1(c), so that $\xi_{-1} = \gamma \cos \omega t$ and $\Delta\theta_0 = \theta_0 - \xi_{-1}/l$, with γ being the driving amplitude, and $f = \omega/2\pi$ the driving frequency.

III. EMISSION OF SOLITONS

Figure 2 shows the process of emission of solitons for $f = 9.33$ Hz and $\gamma = 12.7$ mm [34]. Growing up from a small-amplitude evanescent wave, the localized wave around the ‘‘impurity’’ at site $n = 0$ is resonantly excited and amplified. When its amplitude is large enough, it undergoes some nonlinear instability and a breakup, releasing almost all of the fed energy as a soliton that propagates away from the ‘‘impurity.’’ The soliton appears as a collective vibration of a group of pendulums whose amplitudes are modulated spatially. After traveling through the chain of 60 sites, it collides on the other

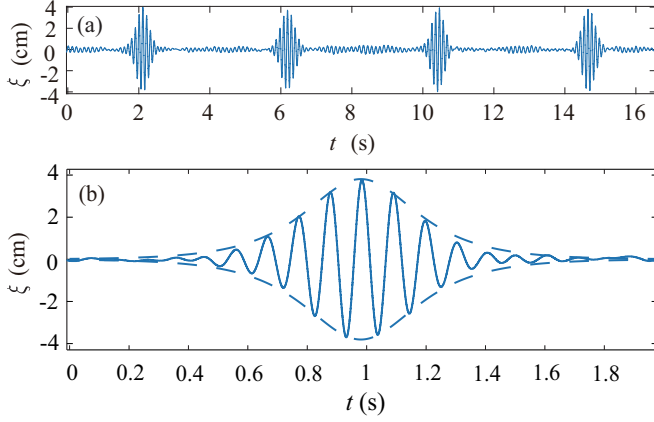


FIG. 3. Detected signal of the displacement of the bob at site $n = 13$ when the drive works at $f = 9.33$ Hz and $\gamma = 12.7$ mm. (a) An overview of the recorded waveform; (b) the magnified view (solid line) of the second wave packet in (a) along with its theoretical hyperbolic secant envelope (dashed line) obtained by using Eq. (8) with the fitting parameter a .

end and is reflected. It finally decays and submerges into the background noise. Once a soliton is released, the localized wave absorbs and accumulates energy from the drive again, and the emission process is repeated. Another noticeable fact is that when the localized wave begins to split, the oscillation of “impurity” changes from out-of-phase to in-phase with the driving [see Fig. 2(c)] until a new soliton completely splits apart. The periodic emission of solitons during the jump between out-of-phase state and in-phase state resembles the Rabi cycle in two-state quantum system.

Figure 3(a) presents a waveform of the displacement ξ_n of the pendulum ball at site $n = 13$, which is detected by an optical sensor, the Laser Displacement Sensor HG-C1200. A magnified view of the second wave packet in this waveform is shown in Fig. 3(b), which exhibits a perfect shape of envelope soliton in agreement with the theoretical sech envelope calculated by Eq. (8). In this experiment, the driving amplitude $\gamma = 12.7$ mm, but the emitted solitons have a much larger amplitude (≈ 40 mm), manifesting the magnification effect and the high efficiency of this type of soliton creation.

According to the waveform, the displacement ξ_n of the vibration assumes the form

$$\xi_n = l\theta_n = (-1)^n \eta(x_n, t) e^{j\omega t} + \text{c.c.} \quad (n = 1, 2, \dots), \quad (6)$$

where $j = \sqrt{-1}$, $x_n = nd$, c.c. denotes the complex conjugate of the term ahead, and $\eta(x, t)$ is the envelope function that modulates the amplitudes of vibration. In long-wave approximation, it is readily derived from Eq. (3) that η is governed by

$$2j\omega \frac{\partial \eta}{\partial t} + \frac{\omega_0^2 d^2}{4} \frac{\partial^2 \eta}{\partial x^2} + \left(\omega_0^2 + \frac{24K_3}{Md^2} |\eta|^2 - \omega^2 \right) \eta = 0. \quad (7)$$

This is a nonlinear Schrödinger equation [30] that admits a traveling single-soliton solution [1,35]

$$\eta(x, t) = a\eta_0 \text{sech} \frac{a}{d} (x - c_s t - x_0) e^{j(k(x - c_s t) + \nu t - \phi_0)}, \quad (8)$$

where $\eta_0 = d\sqrt{K_1/12K_3}$, $c_s = (k/4\omega)(\omega_0 d)^2$, x_0 and ϕ_0 are arbitrary constants, and a is determined by wave number k , driving frequency ω , and an additional frequency ν as

$$a = \sqrt{4(\omega^2 - \omega_0^2 + 2\omega\nu)/\omega_0^2 - (kd)^2}. \quad (9)$$

The solution (8) well describes the experimentally observed soliton that travels along the chain at a speed c_s that is highly relevant to amplitude a .

IV. EMISSION RATE CONTROL

The repeat rate of the emission, f_e , is found to highly depend on the driving parameters, as shown in Fig. 4(a). Since in the experiment $f_0 = \omega_0/2\pi$ is a little lower than the theoretical calculation, we start from the driving frequency $f = 8.70$ Hz and increase it step by step with a fixed driving amplitude $\gamma = 10$ mm. At first, the localized wave mode quickly reaches its nonlinear saturation and becomes unstable, leading to the emission of solitons at a pretty high rate f_e . At a higher f , the localized wave seems to be more robust and absorbs a larger amount of energy from the drive during a longer time period, so that the localized wave has larger amplitude before triggering the nonlinear instability and the emitted soliton has larger amplitude. The rate of emission

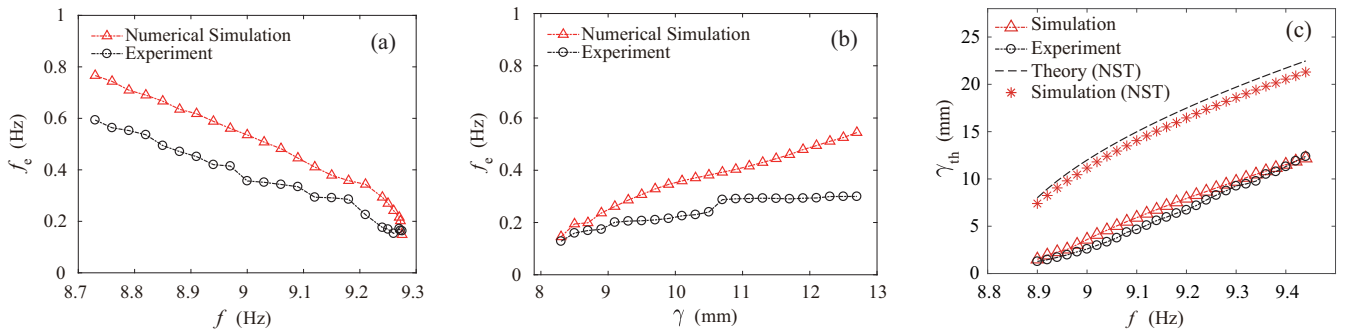


FIG. 4. (a) The emission rate f_e versus the driving frequency f with fixed $\gamma = 10$ mm. (b) The emission rate f_e versus the driving amplitude γ with fixed $f = 9.20$ Hz. (c) The threshold of driving amplitude for emission versus the driving frequency. The theoretical and numerical curves of nonlinear supratransmission (NST) are also presented for comparison.

therefore decreases approximately linearly as f is increased. We have also investigated the dependence of the emission rate f_e on driving amplitude γ , with f fixed at 9.20 Hz. Figure 4(b) shows that the emission rate f_e increases with γ , which is in line with our physical intuition. The discrepancy between the numerically computed and the experimentally measured in Figs. 4(a) and 4(b) is attributed to the damping effect. Therefore, by tuning the (f, γ) parameters, we can control the emission of solitons, even at an extremely low rate so that there is only one soliton traveling back and forth along the finite lattice of pendulums before a new one is generated.

For a given driving frequency f , there is a threshold of driving amplitude γ , denoted by γ_{th} , below which the fed energy is insufficient to have the localized wave undergo a nonlinear instability and the localized wave will keep stationary. For $\gamma > \gamma_{th}$ but in close proximity to γ_{th} , solitons are emitted at an extremely low rate. The existence of γ_{th} at $f \approx f_r$ should be totally ascribed to the inevitable damping dissipation. γ_{th} , of course, is frequency dependent. This dependency is measured and presented in Fig. 4(c), which is in a good agreement with the numerically calculated before [30]. Compared with supra-

transmission (without the “impurity”), the driving threshold has been significantly reduced.

V. CONCLUSION

In conclusion, we have presented an experimental demonstration of emission of solitons by the resonance of a localized wave. We also demonstrate the controllability of the emission process via tuning the driving parameters, which provides great convenience for practical applications. Another attracting feature is the high efficiency of soliton creation in that most of the energy accumulated in the localized wave is converted to solitons, making it possible to generate pure and large-amplitude solitons by using a weak drive. We believe that the proposed mechanism is generalizable to other nonlinear wave systems for efficient and controllable generation of solitons.

ACKNOWLEDGMENT

This work was supported by the National Science Foundation of China under Grants No. 11574149, No. 11174140, and No. 10874085.

-
- [1] M. Remoissenet, *Waves Called Solitons: Concepts and Experiments* (Springer-Verlag, New York, 1999).
 - [2] R. Trines, R. Bingham, M. W. Dunlop, A. Vaivads, J. A. Davies, J. T. Mendonça, L. O. Silva, and P. K. Shukla, *Phys. Rev. Lett.* **99**, 205006 (2007).
 - [3] G. M. Reznik and V. Zeitlin, *Phys. Rev. Lett.* **96**, 034502 (2006).
 - [4] D. Farmer and L. Armi, *Science* **283**, 188 (1999).
 - [5] J. Wu, R. Keolian, and I. Rudnick, *Phys. Rev. Lett.* **52**, 1421 (1984).
 - [6] J. Denschlag, J. E. Simsarian, D. L. Feder, C. W. Clark, L. A. Collins, J. Cubizolles, L. Deng, E. W. Hagley, K. Helmerson, W. P. Reinhardt *et al.*, *Science* **287**, 97 (2000).
 - [7] K. E. Strecker, G. B. Partridge, A. G. Truscott, and R. G. Hulet, *Nature (London)* **417**, 150 (2002).
 - [8] M. Wu, B. A. Kalinikos, and C. E. Patton, *Phys. Rev. Lett.* **93**, 157207 (2004).
 - [9] I. Kourakis, N. Lazarides, and G. P. Tsironis, *Phys. Rev. E* **75**, 067601 (2007).
 - [10] P. J. Reece, E. M. Wright, and K. Dholakia, *Phys. Rev. Lett.* **98**, 203902 (2007).
 - [11] B. Damski and W. H. Zurek, *Phys. Rev. Lett.* **104**, 160404 (2010).
 - [12] E. Bourdin, J.-C. Bacri, and E. Falcon, *Phys. Rev. Lett.* **104**, 094502 (2010).
 - [13] M. Sich, D. Krizhanovskii, M. Skolnick, A. V. Gorbach, R. Hartley, D. V. Skryabin, E. Cerda-Méndez, K. Biermann, R. Hey, and P. Santos, *Nat. Photon.* **6**, 50 (2012).
 - [14] E. A. Cerda-Méndez, D. Sarkar, D. N. Krizhanovskii, S. S. Gavrilov, K. Biermann, M. S. Skolnick, and P. V. Santos, *Phys. Rev. Lett.* **111**, 146401 (2013).
 - [15] F. Leo, S. Coen, P. Kockaert, S.-P. Gorza, P. Emplit, and M. Haelterman, *Nat. Photon.* **4**, 471 (2010).
 - [16] T. Herr, V. Brasch, J. D. Jost, C. Y. Wang, N. M. Kondratiev, M. L. Gorodetsky, and T. J. Kippenberg, *Nat. Photon.* **8**, 145 (2014).
 - [17] S. Clarke, R. Grimshaw, P. Miller, E. Pelinovsky, and T. Talipova, *Chaos* **10**, 383 (2000).
 - [18] L. F. Mollenauer, R. H. Stolen, and J. P. Gordon, *Phys. Rev. Lett.* **45**, 1095 (1980).
 - [19] G. I. Stegeman and M. Segev, *Science* **286**, 1518 (1999).
 - [20] L. Friedland and A. G. Shagalov, *Phys. Rev. Lett.* **81**, 4357 (1998).
 - [21] L. Friedland and A. G. Shagalov, *Phys. Rev. Lett.* **90**, 074101 (2003).
 - [22] F. Geniet and J. Leon, *Phys. Rev. Lett.* **89**, 134102 (2002).
 - [23] F. Geniet and J. Leon, *J. Phys.: Condens. Matter* **15**, 2933 (2003).
 - [24] P. Anghel-Vasilescu, J. Dornignac, F. Geniet, J. Leon, and M. Taki, *Phys. Rev. Lett.* **105**, 074101 (2010).
 - [25] P. Anghel-Vasilescu, J. Dornignac, F. Geniet, J. Leon, and A. Taki, *Phys. Rev. A* **83**, 043836 (2011).
 - [26] H. C. Kim, R. L. Stenzel, and A. Y. Wong, *Phys. Rev. Lett.* **33**, 886 (1974).
 - [27] G. J. Morales and Y. C. Lee, *Phys. Fluids* **20**, 1135 (1977).
 - [28] H.-H. Chen and C.-S. Liu, *Phys. Rev. Lett.* **39**, 1147 (1977).
 - [29] J. C. Adam, A. Gourdin Serveniere, and G. Laval, *Phys. Fluids* **25**, 376 (1982).
 - [30] G. Yu, X. Wang, and Z. Tao, *Phys. Rev. E* **83**, 026605 (2011).
 - [31] P. M. Morse and K. U. Ingard, *Theoretical Acoustics* (Princeton University Press, Princeton, 1986).
 - [32] C. Zhu, J. Lei, Y. Wu, N. Li, D. Chen, and Q. Shi, *Eur. J. Phys.* **36**, 045002 (2015).
 - [33] S. Dusuel, P. Michaux, and M. Remoissenet, *Phys. Rev. E* **57**, 2320 (1998).
 - [34] See Supplemental Material at <http://link.aps.org/supplemental/10.1103/PhysRevE.102.052201> for the recorded video of the dynamic process of emission of solitons.
 - [35] Y. S. Kivshar, F. Zhang, and S. Takeno, *Physica D* **113**, 248 (1998).